Differential geometric structures of stream functions: incompressible two-dimensional flow and curvatures

Yamasaki, Kazuhito

Yajima, T.

Iwayama, Takahiro

Differential geometric structures of stream functions: incompressible two-dimensional flow and curvatures

K Yamasaki[1,†], T Yajima[2,‡] and T Iwayama[1,*]

[1] Department of Earth and Planetary Sciences, Faculty of Science, Kobe University, Nada-ku, Kobe 657-8501, Japan

[2] Department of Physics, Faculty of Science, Tokyo University of Science, 1-3 Kagurazaka, Shinjuku-ku, Tokyo, 162-8601, Japan

E-mail: [†]yk2000@kobe-u.ac.jp

E-mail: [‡]t-yajima@rs.kagu.tus.ac.jp

E-mail: [*]iwayama@kobe-u.ac.jp

Abstract. The Okubo-Weiss field, frequently used for partitioning incompressible two-dimensional (2D) fluids into coherent and incoherent regions, corresponds to the Gaussian curvature of the stream function. Therefore, we consider the differential geometric structures of stream functions and calculate the Gaussian curvatures of some basic flows. We find the following. (I) The vorticity corresponds to the mean curvature of the stream function. Thus, the stream-function surface for irrotational flow and parallel shear flow correspond to the minimal surface and a developable surface, respectively. (II) The relationship between the coherency and the magnitude of the vorticity is interpreted by the curvatures. (III) Using the Gaussian curvature, stability of single and double point vortex streets is analyzed. The results of this analysis are compared with the well-known linear stability analysis. (IV) Conformal mapping in fluid mechanics is physical expression of the geometric fact that the sign of the Gaussian curvature does not change in conformal mapping. These findings suggest that the curvatures of stream functions are useful for understanding the geometric structure of incompressible 2D flow.

PACS numbers: 02.40.Hw, 47.10.A-, 47.15.km, 47.32.ck

Submitted to: *J. Phys. A: Math. Gen.*

1. Introduction

To conduct research in the field of geometric theory, it is helpful to identify a relationship between a physical quantity and a geometric quantity. For instance, the general theory of relativity has shown that gravitational potential corresponds to the metric of space-time. In the geometric theory of continuum mechanics, various relationships have been also known. For instance, in solid mechanics, defect fields are recognized as torsion and the Riemann-Cartan curvature of material space-time [1–5]. This geometric approach has been developed on the basis of differential geometry and gauge theory [6–8] and applied in several fields such as solid earth sciences [9–11].

In fluid mechanics, geometric approaches have been applied to various subjects. For example, the Navier-Stokes equations on a Riemannian manifold, and interesting relationships have been proposed [12–15]. Fischer [15] showed that the scalar non-dynamic term of the conformal Ricci flow equation (a geometric quantity) is analogous to the pressure term of the Navier-Stokes equations (a physical quantity). Weiss [16] proposed a field, the so-called Okubo-Weiss field, that is used for partitioning an incompressible two-dimensional (2D) fluid into regions with different dynamic properties. The Okubo-Weiss field has been widely used for analyzing atmospheric and oceanic circulations and realized as an important quantity to characterize flow field (*e.g.* [17, 18]). Moreover, he mentioned that the Okubo-Weiss field corresponds to the Gaussian curvature of the stream function. However, few studies have focused on the Weiss's correspondence, although the Gaussian curvature is known as a fundamental quantity to characterize a surface. From view point of differential geometry, natural questions arise: What is a physical quantity corresponding to the mean curvature of the stream function, which is also one of fundamental quantities for a surface? What types of flow field correspond to the minimal surface (vanishing the mean curvature) and the developable surface (vanishing the Gaussian curvature)? However, these questions have not been considered yet. Thus, the main purpose of this study is to consider the differential geometric structure of the stream function.

In this study, we consider incompressible 2D flow because the stream function can be defined in this case. A correspondence between the mean curvature of the stream function and the vorticity shows that the irrotational flows can be expressed by the minimal surface. We thus focus primarily on irrotational flows (*i.e.*, potential flows). Another aim of this study is to present the curvatures of basic potential flows and their superposition concretely. The concrete forms of the stream functions corresponding to various kinds of basic flows, such as uniform flow, the source-sink, and the point vortex are already known. It is thought that the geometric structure of the stream function is unique for each basic flow. Moreover, superposition of basic flows allow us to obtain more complex flows that describe, for example, the flow around a body with a particular shape of interest. Therefore, it is necessary for the geometric theory of the potential flows to consider the role of curvature in the superposition. We also calculate the curvatures of non-potential flows, such as uniform flow with local symmetry and

Rankine's combined vortex.

In Section 2, we present the theory. We give a brief overview of the Okubo-Weiss field and consider the geometric structure of the stream function. To determine the Gaussian curvature of the steam function for irrotational flow, we derive a Gaussian curvature formula for the stream function in terms of the complex velocity potential. In Section 3, we present the results. Based on the theory in Section 2, we calculate concretely the Gaussian curvatures of some basic potential flows and their superposition. Moreover, we consider single and double vortex streets and Rankine's combined vortex. Section 4 contains a discussion of the results. We discuss the stability of the single and double point vortex streets in terms of the Gaussian curvature of the stream function and the curvatures of the potential and non-potential flows. Moreover, we reconsider the geometric structure of the stream function based on conformal mapping. Section 5 gives our conclusions.

2. Theory

2.1. Brief overview of the Okubo-Weiss field

In this study, we consider incompressible 2D flows. First, we give a brief overview of the Okubo-Weiss field and express it in terms of the stream function.

In freely decaying 2D turbulence governed by the Navier-Stokes equations, it is well known that long-lived, coherent vortices spontaneously emerge from random initial conditions. They evolve through mutual advection, approximately described by Hamiltonian advection of point vortices and the merging of like-signed vortices [19]. Ultimately, they dominate the evolution of the entire system. The quantity Q, proposed by Weiss [16], has been used to extract coherent vortices from a turbulent field. The evolution of incompressible 2D fluids is written in terms of the vorticity using the so-called vorticity equation. To study the deformation of the vorticity, Weiss concentrated on the vorticity gradient. Under the assumption that the velocity gradient tensor slowly varies with respect to the vorticity gradient, he derived a vorticity gradient that evolves exponentially at a rate of $\pm\sqrt{Q}$, where Q is defined by

$$Q = \frac{1}{4}(\sigma^2 - \omega^2), \tag{1}$$

where σ^2 is the square of the rate of strain:

$$\sigma^2 = (\partial_x u - \partial_y v)^2 + (\partial_y u + \partial_x v)^2, \tag{2}$$

and ω is the vorticity:

$$\omega = \partial_x v - \partial_y u. \tag{3}$$

Here, u and v are velocity components in the x and y directions, respectively. The coherent region is defined by the region of the fluid in which $Q < 0$. Equation (1) indicates that the vorticity predominates over the rate of the strain in such regions.

The continuity equation for incompressible 2D flow is given by $\partial_x u + \partial_y v = 0$. This continuity equation is identically satisfied by introducing the stream function, $\psi(x, y)$:

$$u = \partial_y \psi, \tag{4}$$

$$v = -\partial_x \psi. \tag{5}$$

Equations (1) and (3) can be rewritten in terms of the stream function as

$$Q = (\partial_x \partial_y \psi)^2 - (\partial_x \partial_x \psi)(\partial_y \partial_y \psi), \tag{6}$$

and

$$\omega = -\partial_x \partial_x \psi - \partial_y \partial_y \psi = -\Delta \psi, \tag{7}$$

respectively.

The quantity Q can be also interpreted as the stability of the trajectory of the Lagrangian particles immersed in the velocity field, as shown by Okubo [20] and reformulated by Benzi *et al.* [19].‡ In this sense, the quantity Q is frequently referred to as the Okubo-Weiss field. Here, we introduce the interpretation of Q by Benzi *et al.* We let $(\delta x, \delta y)$ be a small perturbation along the trajectories. Within a linear approximation, the perturbation evolves in the following way:

$$\frac{d}{dt} \begin{pmatrix} \delta x \\ \delta y \end{pmatrix} = \begin{pmatrix} \partial_x \partial_y \psi & \partial_y \partial_y \psi \\ -\partial_x \partial_x \psi & -\partial_x \partial_y \psi \end{pmatrix} \begin{pmatrix} \delta x \\ \delta y \end{pmatrix}. \tag{8}$$

Therefore, the evolution of the perturbation on the particle at the initial position (x_0, y_0) is given by

$$\begin{pmatrix} \delta x(t) \\ \delta y(t) \end{pmatrix} = \begin{pmatrix} \delta x(0) \\ \delta y(0) \end{pmatrix} \exp(\Lambda t), \tag{9}$$

where Λ are the eigenvalues of the matrix (8):

$$\Lambda = \pm \sqrt{Q}. \tag{10}$$

Here, Q in (10) is evaluated at $(x_0,\, y_0)$.

From (9) and (10), the sign of Q is related to the evolution of the distance between two Lagrangian particles embedded in the velocity field (4) and (5) [19]. For instance, in the region of the fluid in which $Q < 0$, the distance between two particles will not diverge exponentially. Thus, the coherent regions are defined as regions in which $Q < 0$ [19], and the definition of the coherent region in terms of Q is referred to as the Okubo-Weiss criterion.

Equation (6) implies that the Okubo-Weiss field Q is determined by the geometric structure of the stream-function surface, $\psi(x, y)$ [16]. We reconsider the Okubo-Weiss field from the perspective of differential geometry, as discussed in the next section.

‡ Okubo [20] discussed 2D flows with velocity singularities such as convergence and divergence. However, Benzi *et al.* [19] investigated non-divergent 2D flows.

2.2. Geometric structure of the stream-function surface

2.2.1. The Okubo-Weiss field, vorticity, and curvatures of the stream-function surface Typically, the geometric structure of a surface is characterized by two curvatures, a Gaussian curvature and a mean curvature [21]. These curvatures can be used to express the geometric structure of the stream-function surface, $\psi(x, y)$.

We let $\psi(x, y)$ be a surface in three-dimensional Euclidean space $\mathbb{R}^3$ and assume that M is the matrix of the second fundamental form:

$$M = \begin{pmatrix} \partial_x\partial_x\psi & \partial_x\partial_y\psi \\ \partial_x\partial_y\psi & \partial_y\partial_y\psi \end{pmatrix}. \tag{11}$$

The determinant and trace of (11) give the Gaussian curvature, K, and the mean curvature, H, of $\psi(x, y)$, respectively:

$$K = \det M = \partial_x\partial_x\psi\partial_y\partial_y\psi - (\partial_x\partial_y\psi)^2, \tag{12}$$

$$2H = \mathrm{tr}M = \partial_x\partial_x\psi + \partial_y\partial_y\psi = \triangle\psi. \tag{13}$$

From (6) and (12), the Gaussian curvature of the stream function is the negative Q value:

$$K = -Q. \tag{14}$$

This relationship was previously identified by Weiss [16]. In contrast, we find from (7) and (13) that the vorticity is twice the negative mean curvature:

$$2H = -\omega. \tag{15}$$

The sign of the vorticity indicates the direction of rotation; thus, the degree of the vorticity is related to the absolute value of H.

We let p be a point on the surface, $\psi(x, y)$. In differential geometry, it is known that the following definitions: (i) p is elliptic if $K(p) > 0$; (ii) p is hyperbolic if $K(p) < 0$; (iii) p is parabolic if $K(p) = 0$, but $M(p) \neq 0$; and (iv) p is planar if $K(p) = 0$ and $M(p) = 0$. Therefore, from (14), the relationship between the physical concepts in fluid mechanics and the geometric concepts in differential geometry is given by

(I) Coherent ($Q < 0$) $\leftrightarrow$ elliptic ($K > 0$);

(II) Incoherent ($Q > 0$) $\leftrightarrow$ hyperbolic ($K < 0$);

(III) Marginal ($Q = 0$) $\leftrightarrow$ parabolic or planar ($K = 0$).

Because the stream function is defined for various 2D flows, we calculate the Gaussian curvatures of the flows, as discussed in section 3.

2.2.2. Plane potential flow and Gaussian curvature It is well known that for an irrotational flow, the velocity potential, ϕ, can be introduced, according to (3), as follows:

$$u = \partial_x \phi, \tag{16}$$

$$v = \partial_y \phi. \tag{17}$$

This type of flow is called potential flow. Equation (15) showed that the mean curvature vanishes in potential flow. This type of surface is called a minimal surface in differential geometry. When $H = 0$, it can be mathematically shown that $K \leq 0$. Indeed, the quantity Q is less than or equal to zero when $\omega = 0$, as shown by (1). Therefore, in the case of (II) and (III) from the previous section, the another relationship between the physical concept in fluid mechanics and the geometric concept in differential geometry is given by

(IV) Potential flow ($\omega = 0$ and $Q \geq 0$) $\leftrightarrow$ minimal surface ($H = 0$ and $K \leq 0$).

In this section, we discuss the geometric structure of potential flow. From (4), (5), (16), and (17), the two functions ψ and ϕ satisfy the Cauchy-Riemann differential equations:

$$\partial_x \phi = \partial_y \psi, \tag{18}$$

$$\partial_y \phi = -\partial_x \psi. \tag{19}$$

The velocity potential surface, $\phi(x, y)$, also exhibits curvatures. However, the Cauchy-Riemann equations show that these curvatures are equal to those of the stream-function surface $\psi(x, y)$. Therefore, in this paper, we focus on the curvatures of $\psi(x, y)$.

For potential flows, we can define the holomorphic function as the complex velocity potential:

$$W = \phi + i\psi. \tag{20}$$

The potential, W, is important in the analysis of potential flow, because various physical quantities can be derived by the differentiation of W. For instance, the velocity is given by

$$\frac{dz}{dt} = u + iv = \frac{d\,\overline{W}}{d\overline{z}}, \tag{21}$$

where $z = x + iy$, and the overbar denotes the complex conjugate.

We derive the relationship between W and the Gaussian curvature. For this, we rewrite (6) in terms of W. From (21) and its complex conjugate, we obtain

$$\frac{d}{dt}\begin{pmatrix} \delta z \\ \delta \overline{z} \end{pmatrix} = \begin{pmatrix} 0 & \frac{d^2\overline{W}}{d\overline{z}^2} \\ \frac{d^2 W}{dz^2} & 0 \end{pmatrix} \begin{pmatrix} \delta z \\ \delta \overline{z} \end{pmatrix}. \tag{22}$$

Therefore, the evolution of $(\delta z, \delta\overline{z})^T$ is given by

$$\begin{pmatrix} \delta z(t) \\ \delta\overline{z}(t) \end{pmatrix} = \begin{pmatrix} \delta z(0) \\ \delta\overline{z}(0) \end{pmatrix} e^{\pm\sqrt{Q}t} \tag{23}$$

with

$$Q = \frac{d^2W}{dz^2}\frac{d^2\overline{W}}{d\overline{z}^2} = \left|\frac{d^2W}{dz^2}\right|^2. \tag{24}$$

Therefore, from (14), we have

$$K = -\left|\frac{d^2W}{dz^2}\right|^2. \tag{25}$$

This shows that $K \leq 0$ in potential flow, as expected from (1) and (14). The formulas (24) and (25) are useful because Q and K can be calculated without extracting the imaginary part of the complex velocity potential.

The concrete curvatures for various potential flows are shown in Section 3.1.

2.3. Superposition and curvatures

An advantage of potential flow is that the stream function for complex flows can be obtained by the superposition of stream functions for relatively simple flows. For instance, we combine simple flows described by ψ_A and ψ_B to obtain a complex flow described by

$$\psi = \psi_A + \psi_B. \tag{26}$$

In this section, we discuss the effect of this superposition on the Gaussian curvatures.

We let K_A and K_B be the Gaussian curvatures of ψ_A and ψ_B, respectively. From (12), the curvature of ψ is given by:

$$K = K_A + K_B + K_I, \tag{27}$$

where

$$K_I = \partial_x\partial_x\psi_A\partial_y\partial_y\psi_B + \partial_x\partial_x\psi_B\partial_y\partial_y\psi_A - 2(\partial_x\partial_y\psi_A)(\partial_x\partial_y\psi_B), \tag{28}$$

or, from (4) and (5),

$$K_I = -\partial_x v_A\partial_y u_B - \partial_x v_B\partial_y u_A - 2(\partial_x u_A)(\partial_x u_B). \tag{29}$$

Here, $(u_A,\, v_A) = (\partial_y\psi_A,\, -\partial_x\psi_A)$ and $(u_B,\, v_B) = (\partial_y\psi_B,\, -\partial_x\psi_B)$. In general, $K_I \neq 0$, *i.e.,* $K \neq K_A + K_B$, so the superposition of the Gaussian curvatures does not necessarily hold true. K_I indicates the interaction between the surfaces ψ_A and ψ_B. This interacting curvature plays an interesting role in the superposition of basic flows. On the other hand, from (13), the superposition of the mean curvature holds true.

Now, instead of the addition given by Equation (26), we consider the subtraction $\psi_A - \psi_B$. This corresponds to the volume flow rate between the two streamlines. In a similar fashion described above, the curvature of the volume flow rate is $K_A + K_B - K_I$.

The concrete curvatures for superposition of basic flows are shown in Sections 3.2 and 3.3.

2.4. Developable surface and parallel shear flow

In Section 2.2.2, we showed that the stream-function surface for potential flows corresponds to a minimal surface: $H = 0$ and $K \neq 0$. This raises the question of which flow corresponds to a developable surface, $H \neq 0$ and $K = 0$, that can be flattened onto a plane without distortion.

The stability problem of parallel shear flow, $(u, v) = (U(y), 0)$, has been a central issue in fluid dynamics [22]. From (1), (2), and (3), the Gaussian curvature for parallel shear flow vanishes. Therefore, the curvatures for parallel shear flow satisfy the conditions $H \neq 0$ and $K = 0$, indicating that the stream-function surface for the parallel shear flow is a developable surface.

3. Results

3.1. Basic plane potential flows

Potential flows can be described by the complex velocity potential, W. Because W is a solution to Laplace's equation, W is a harmonic (holomorphic) function. The concrete forms of the harmonic functions correspond to the various basic flows. As mentioned for case (IV) in Section 2.2.2, only the non-positive Gaussian curvature characterizes the potential flow. In this section, we present calculations of the non-positive K related to basic potential flows, *i.e.*, the harmonic functions. The significance of the results will be discussed in Section 4.

3.1.1. Uniform flow The simplest plane flow is one for which the streamlines are all straight and parallel, and the magnitude of the velocity is constant [23]. This corresponds to uniform flow. The complex velocity potential, W, of uniform flow is given by the following harmonic function:

$$W(z) = Ue^{-i\alpha}z, \tag{30}$$

where U is the magnitude of the velocity and α is the angle of attack, i.e., the angle of the flow relative to the x axis (Fig. 1(a)).

From $z = x + iy$ and Euler's formula, the stream function is given by

$$\psi = \Im[W] = U(y\cos\alpha - x\sin\alpha), \tag{31}$$

where $\Im$ denotes the imaginary part of W. In this case, the matrix (11) becomes zero, so the Gaussian curvature is also zero. That is, the stream function of the uniform flow is planar.

The constant α in (30) or (31) indicates the global symmetry of the system. Following gauge theory, this symmetry can be localized by replacing α with $\alpha(x)$:

$$\psi = U(y\cos\alpha(x) - x\sin\alpha(x)). \tag{32}$$

Note that this is not potential flow, so W cannot be defined. From (12) and (13), the Gaussian and the mean curvatures of this flow are

$$K = -(U\alpha' \sin\alpha)^2, \tag{33}$$

$$2H = -U\{2\alpha' \cos\alpha + (y\cos\alpha - x\sin\alpha)(\alpha')^2 + (x\cos\alpha + y\sin\alpha)\alpha''\}. \tag{34}$$

3.1.2. Corner flow and source doublet We consider the power law potential:

$$W(z) = Az^n, \tag{35}$$

where $A(> 0)$ is a scaling parameter, and the exponent $n(\neq 0)$ characterizes various flows. For instance, positive n describes the flow around or through a corner (Figs. 1(b) and (c)). The case of $n = -1$ gives the flow due to a source doublet (Fig. 1(d)).

From $z = re^{i\theta}$, the stream function in terms of x and y is given by

$$\psi = \Im[W] = A(x^2 + y^2)^{n/2} \sin\left\{n \arctan\left(\frac{y}{x}\right)\right\}. \tag{36}$$

Therefore, from (12), the Gaussian curvature is

$$K = -A^2(n-1)^2 n^2 (x^2 + y^2)^{n-2}. \tag{37}$$

This curvature varies with the value of $n(> 0)$, *i.e.*, the angle of the corner flow. When $n = 1$, the angle is π (*i.e.*, uniform flow), so the curvature vanishes, as described in Section 3.1.1.

3.1.3. Source and sink For the radial flow shown in Fig. 1(e), the complex velocity potential, W, is given by

$$W(z) = \frac{m}{2\pi} \log z, \tag{38}$$

where m is the flow rate. If m is positive, the flow is radially outward, *i.e.*, a source flow. If m is negative, the flow is toward the origin, *i.e.*, a sink flow.

The stream function is given by

$$\psi = \Im[W] = \frac{m}{2\pi} \arctan\left(\frac{y}{x}\right). \tag{39}$$

Therefore, from (12), the Gaussian curvature is

$$K = -\left\{\frac{m}{2\pi(x^2 + y^2)}\right\}^2. \tag{40}$$

Note that the position of the source or the sink, $(x, y) = 0$, is a singular point. Thus, the velocity and the Gaussian curvature at this point cannot be defined.

3.1.4. Point vortex We consider flow in which the streamlines are concentric circles, *i.e.*, a flow field induced by a point vortex, as shown in Fig. 1(f). In this case, the complex velocity potential, W, is given by

$$W(z) = -\frac{i\Gamma}{2\pi}\log z, \tag{41}$$

where Γ is the strength of the point vortex. If Γ is positive (negative), the vortex induces counterclockwise (clockwise) motion around the point vortex. The stream function is given by

$$\psi = \Im[W] = -\frac{\Gamma}{4\pi}\log(x^2+y^2). \tag{42}$$

Therefore, from (12), the Gaussian curvature is

$$K = -\left\{\frac{\Gamma}{2\pi(x^2+y^2)}\right\}^2. \tag{43}$$

Note that one should not apply (43) at the position of the vortex, $(x, y) = 0$. It is known that the point vortex does not induce the velocity at its position. To calculate the velocity and the Gaussian curvature of the stream function for the point vortex at the position of the vortex, the complex velocity potential, W', must be used without the effect of self-interaction. In the present case, this velocity potential is $W' = 0$. Therefore, the velocity at $(x, y) = 0$ is given by

$$u(0) + iv(0) = \left.\frac{\mathrm{d}\overline{W'}}{\mathrm{d}\overline{z}}\right|_{(x,y)=0} = 0. \tag{44}$$

Moreover, the Gaussian curvature of the stream function at $(x, y) = 0$ is

$$K(0) = \left.\left|\frac{\mathrm{d}^2W'}{\mathrm{d}z^2}\right|^2\right|_{(x,y)=0} = 0. \tag{45}$$

3.2. Superposition of basic plane potential flows

We obtain more complex flows by the superposition of basic flows. Because any streamline in an inviscid flow can be considered a solid boundary, superposition can be used to describe the flow around a body with a particular shape of interest [23]. In this section, we focus on three classical examples of basic flow superposition.

3.2.1. Source in a uniform stream: A half-body We obtain the flow around a half-body by adding a source, (38), to a uniform flow, (30), parallel to the x-axis (Fig. 2(a)):

$$W(z) = Uz + \frac{m}{2\pi}\log z. \tag{46}$$

The stream function is given by

$$\psi = \Im[W] = Uy + \frac{m}{2\pi}\arctan\left(\frac{y}{x}\right). \tag{47}$$

Therefore, from (27) and (28), the Gaussian curvature, except for $(x, y) = 0$, is

$$K = -\left\{\frac{m}{2\pi(x^2+y^2)}\right\}^2. \tag{48}$$

Because the curvature related to the uniform flow is zero, only the curvature related to the source remains. Similar to the source and sink flows, the position $(x, y) = 0$ is a singular point of the flow. Thus, the Gaussian curvature cannot be defined at this point.

We consider the Gaussian curvature at the stagnation point. The velocity of the flow around a half-body consists of the velocity superposition of the basic flows $u = U + (m/2\pi)\{x/(x^2+y^2)\}$ and $v = (m/2\pi)\{y/(x^2+y^2)\}$, where we use (4) and (5). From $(u, v) = (0, 0)$, the position of the stagnation point is $(x, y) = (-m/(2\pi U), 0)$. Therefore, the Gaussian curvature at the stagnation point is given by

$$K|_{u=v=0} = -\left(\frac{2\pi U^2}{m}\right)^2 = -\left(\frac{2\pi U}{D}\right)^2, \tag{49}$$

where $D \equiv m/U$ is the thickness of the half-body.

3.2.2. Doublet in a uniform stream: A circular cylinder We obtain the flow around a circular cylinder by adding a doublet, (35), with $n = -1$, to the uniform flow, (30), parallel to the x-axis (Fig. 2(b)):

$$W(z) = Uz + \frac{A}{z}. \tag{50}$$

The stream function is given by

$$\psi = \Im[W] = \left(U - \frac{A}{r^2}\right) y = \left(U - \frac{A}{x^2+y^2}\right) y. \tag{51}$$

Therefore, from (27) and (28), the Gaussian curvature is

$$K = -\frac{4A^2}{(x^2+y^2)^3}. \tag{52}$$

Only the Gaussian curvature that relates to the doublet remains.

The velocity of the flow consists of the velocity superposition of the basic flows. Therefore, we estimate the radius of the cylinder, a, from $(u, v) = (0, 0)$; *i.e.*, $\sqrt{x^2+y^2} = a = \sqrt{A/U}$. Therefore, the Gaussian curvature on the radius of the cylinder is given by

$$K|_{u=v=0} = -\frac{4U^3}{A}. \tag{53}$$

3.2.3. Doublet and point vortex in a uniform stream: A rotating cylinder We obtain the flow around a rotating cylinder by adding the point vortex of strength, Γ, (41), to the combined potential, (50) (Fig. 2(c)):

$$W(z) = U\left(z + \frac{a^2}{z}\right) + \frac{i\Gamma}{2\pi}\log\left(\frac{z}{a}\right), \tag{54}$$

where a is the radius of the cylinder defined in the previous section. We modified the term of the point vortex for $\psi = 0$ on $z = a$. The stream function is given by

$$\psi = \Im[W] = U\left(1 - \frac{a^2}{x^2+y^2}\right)y + \frac{\Gamma}{2\pi}\log\left(\frac{\sqrt{x^2+y^2}}{a}\right). \tag{55}$$

Therefore, from (27) and (28), the Gaussian curvature is

$$K = -\frac{4a^4U^2}{(x^2+y^2)^3} - \frac{\Gamma^2}{4\pi^2(x^2+y^2)^2} - \frac{2a^2Uy\Gamma}{\pi(x^2+y^2)^3}. \tag{56}$$

The first term is the curvature when only the flow around the cylinder exists (52). The second term is the curvature when only the point vortex exists (43). The third term is the curvature caused by the interaction between the flow around the cylinder and the point vortex.

The location of the stagnation point for the rotating cylinder depends on the inequality between Γ and $4a\pi U$. That is, there exist two stagnation points on the circumference of the circle for $\Gamma < 4a\pi U$, and one stagnation point inside the flow for $\Gamma > 4a\pi U$. In those cases, K is negative. As Γ increases, the two stagnation points on the boundary of the circle approach each other and coalesce at the point $(0, -a)$ when Γ becomes equal to $4a\pi U$. This critical case corresponds to the vanishing point of the total curvature:

$$K = 0, \tag{57}$$

because the solution of this equation is given by

$$y = \frac{-4a^2\pi U \pm ix\Gamma}{\Gamma}. \tag{58}$$

This shows that the real solution for (57) exists at the point $(0, -a)$ for $\Gamma = 4a\pi U$.

3.3. Vortex street

3.3.1. Single vortex street We consider a row of point vortices along the x-axis (Fig. 3(a)). The strength of the vortices is Γ, and the distances, b, between the vortices are the same. The complex potential of such a street is given by the superposition of point vortices, (41):

$$
\begin{aligned}
W(z) &= \sum_{n=-\infty}^{\infty} -\frac{i\Gamma}{2\pi}\log(z+nb) \\
&= -\frac{i\Gamma}{2\pi}\left[\log z + \log\left\{\tilde{A}\,\Pi_{n=1}^{\infty}\left(1-\frac{z^2}{n^2b^2}\right)\right\}\right] \\
&= -\frac{i\Gamma}{2\pi}\log\left(\sin\frac{\pi z}{b}\right) + \tilde{B},
\end{aligned} \tag{59}
$$

where we use the formula $(\sin\pi z)/(\pi z) = \Pi_{n=1}^{\infty}(1-z^2/n^2)$, and $\tilde{A}$ and $\tilde{B}$ are values that are independent of z. Because it is difficult to extract the imaginary part of W (*i.e.*, the stream function), we calculate the Gaussian curvature directly using (25):

$$
K = -\left\{\frac{\pi\Gamma}{b^2(\cos\frac{2\pi x}{b} - \cosh\frac{2\pi y}{b})}\right\}^2. \tag{60}
$$

This shows that the Gaussian curvature located far away from the vortex street is given by

$$
K|_{y\to\pm\infty} = 0. \tag{61}
$$

That is, the flow approaches a uniform flow.

The Gaussian curvature along the vortex street, *i.e.*, the x-axis, and, except for the positions of the point vortices ($x \neq nb$, $y = 0$, where n is an integer), is given by

$$
K|_{y=0} = -\left\{\frac{\pi\Gamma}{b^2(\cos\frac{2\pi x}{b} - 1)}\right\}^2. \tag{62}
$$

To evaluate the Gaussian curvature at the positions of the point vortices (*i.e.*, $z = nb$), we extract the effect of the vortices at the points of interest, as explained in Section 3.1.4. We derive the Gaussian curvature at the origin, $z = 0$. Because the vortex distribution is symmetric along the $x-$axis, the Gaussian curvature at $z = nb$, $(n \neq 0)$ equals that at $z = 0$. The complex velocity potential, $\tilde{W}$, without the self-interaction effect of the vortex at $z = 0$, is given by

$$
\tilde{W}(z) = -\frac{i\Gamma}{2\pi}\log\left(\frac{\sin\frac{\pi z}{b}}{\frac{\pi z}{b}}\right). \tag{63}
$$

In the vicinity of $z = 0$, we can express the complex velocity as

$$
\frac{d\tilde{W}}{dz} = -\frac{i\Gamma}{2b}\frac{\frac{\pi z}{b}\cos\frac{\pi z}{b} - \sin\frac{\pi z}{b}}{\frac{\pi z}{b}\sin\frac{\pi z}{b}} \tag{64}
$$

$$
= \frac{i\Gamma\pi}{6b^2}z + \mathcal{O}(z^2). \tag{65}
$$

Because $d\tilde{W}/dz = u - iv$, the induced velocity at $z = 0$ becomes zero. Moreover, from (25), the Gaussian curvature at $z = 0$ is given by

$$
K(0) = -\frac{\pi^2\Gamma^2}{36b^4}. \tag{66}
$$

3.3.2. Double vortex street By extending the theory of the single vortex street, we consider two parallel rows of point vortices, *i.e.*, Kármán vortex (Fig. 3(b)). In this case, the strengths of the point vortices in rows A and B are Γ and $-\Gamma$, respectively. As shown in Fig. 3(b), d is the distance between the rows, and c is the distance in the direction of x, toward which the vortices in row B shift from those in row A. The complex velocity potential of this double street is given by the following superposition:

$$W = W_A + W_B, \tag{67}$$

$$W_A = -\frac{i\Gamma}{2\pi}\log\left(\sin\frac{\pi z}{b}\right), \tag{68}$$

$$W_B = \frac{i\Gamma}{2\pi}\log\left(\sin\frac{\pi(z-z_0)}{b}\right), \tag{69}$$

where W_A and W_B are the complex velocity potentials for rows A and B, respectively, and $z_0 = c + id$. Thus, the total complex potential is

$$W = -\frac{i\Gamma}{2\pi}\log\left\{\frac{\sin\frac{\pi z}{b}}{\sin\frac{\pi(z-z_0)}{b}}\right\}. \tag{70}$$

From (25), the Gaussian curvature of the double vortex street is given by

$$K = -\left|\frac{\Gamma\pi}{2b^2}\frac{\sin\frac{\pi(2z-z_0)}{b}\sin\frac{\pi z_0}{b}}{\left\{\sin\frac{\pi z}{b}\sin\frac{\pi(z-z_0)}{b}\right\}^2}\right|^2. \tag{71}$$

Similar to the previous subsection, we evaluate the Gaussian curvature at the positions of the vortices, *i.e.*, $z = nb$ and $z = nb + z_0$. Now, we discuss the Gaussian curvature at $z = 0$. The complex velocity potential without the self-interaction effect of the vortex at $z = 0$ is given by

$$\tilde{W}(z) = -\frac{i\Gamma}{2\pi}\log\left\{\frac{\sin\frac{\pi z}{b}}{\frac{\pi z}{b}\sin\frac{\pi(z-z_0)}{b}}\right\}. \tag{72}$$

Thus, in the vicinity of $z = 0$, we obtain

$$\frac{d\tilde{W}}{dz} = -\frac{i\Gamma}{2b}\frac{\frac{\pi z}{b}\sin\frac{\pi z_0}{b} + \sin\frac{\pi z}{b}\sin\frac{\pi(z-z_0)}{b}}{\frac{\pi z}{b}\sin\frac{\pi z}{b}\sin\frac{\pi(z-z_0)}{b}} \tag{73}$$

$$= \frac{i\Gamma}{2b}\left\{\cot\frac{\pi z_0}{b} + \left(\frac{2}{3} + \cot^2\frac{\pi z_0}{b}\right)\frac{\pi z}{b}\right\} + \mathcal{O}(z^2). \tag{74}$$

Therefore, the induced velocity at $z = 0$ is given by

$$u(0) - iv(0) = \frac{i\Gamma}{2b}\cot\frac{\pi z_0}{b} \tag{75}$$

$$= \frac{\Gamma}{2b}\frac{\sinh\frac{2\pi d}{b} + i\sin\frac{2\pi c}{b}}{\cosh\frac{2\pi d}{b} - \cos\frac{2\pi c}{b}}. \tag{76}$$

When $v = 0$, we obtain the well-known double-street configuration: the symmetric arrangement ($c = 0$) or the staggered arrangement ($c = b/2$).

From (25), the Gaussian curvature at $z = 0$ is given by

$$K(0) = -\left|\frac{i\Gamma\pi}{2b^2}\left(\frac{2}{3} + \cot^2\frac{\pi z_0}{b}\right)\right|^2. \tag{77}$$

Because of the symmetry of the configuration of the vortex street and the Gaussian curvature dependence on Γ^2, (77) is valid for the position $z = 0$ as well as the positions of the vortices, $z = nb$ and $z = nb + z_0$.

In Section 4.4, we discuss the stability of the street and the curvature.

3.4. Rankine's combined vortex

Rankine's combined vortex is a circular vortex that has a constant vorticity distribution within a radius as a central core and an irrotational flow distribution outside the core. We let r_0 be the radius of the central core. In this case, the stream functions inside and outside the core are given as follows, respectively:

$$\psi_{r\le r_0} = -\frac{\omega}{4}r^2, \tag{78}$$

$$\psi_{r\ge r_0} = -\frac{\omega}{2}(r_0)^2\log\frac{r}{r_0} - \frac{\omega}{4}(r_0)^2. \tag{79}$$

Then, the Gaussian and mean curvatures inside the core are given by

$$K_{r\le r_0} = \frac{\omega^2}{4} > 0, \tag{80}$$

$$H_{r\le r_0} = -\frac{\omega}{2} \neq 0, \tag{81}$$

and those outside the core are given by

$$K_{r\ge r_0} = -\frac{(r_0)^4\omega^2}{4r^4} < 0, \tag{82}$$

$$H_{r\ge r_0} = 0. \tag{83}$$

4. Discussion

4.1. Geometric interpretation of the relationship between the Okubo-Weiss field and vorticity

In this study, we focused on incompressible 2D flow described by the stream function. The Okubo-Weiss field, which is frequently used to define the coherent region in this flow, corresponds to the Gaussian curvature of the stream-function surface, $\psi(x, y)$. In this paper, we pointed out that the vorticity corresponds to the mean curvature of $\psi(x, y)$. In differential geometry, it is well known that a surface can be characterized by the mean and Gaussian curvatures. Therefore, the correspondences found by Weiss [16]

and this study suggest that the stream-function surface can be characterized by the vorticity and the the Okubo-Weiss field.

The Okubo-Weiss field is not independent of the vorticity [19, 24], which is related to the fact that the Gaussian curvature is not independent of the mean curvature. The values of $|\omega|$ in the negative Q regions are generally large compared to those in the positive Q regions [16, 19, 24]. (14) showed that $K = -Q$, and (15) showed that $2H = -\omega$. These physical relationships can be interpreted geometrically as follows: $|H|$ in the regions with $K > 0$ are generally large compared to those in the regions with $K < 0$. Next, we discuss the validity of this relationship.

For this discussion, we introduce the principal curvatures κ_1 and κ_2 by choosing an orthonormal basis of eigenvectors of the matrix (11). Moreover, using (12) and (13), the matrix (11) can be diagonalized as

$$N = \begin{pmatrix} \kappa_1 & 0 \\ 0 & \kappa_2 \end{pmatrix}, \tag{84}$$

where $\kappa_1 = H + \sqrt{H^2 - K}$ and $\kappa_2 = H - \sqrt{H^2 - K}$. Therefore, the Gaussian curvature and the mean curvature in terms of κ_1 and κ_2 are given by

$$K = \det N = \kappa_1 \kappa_2, \tag{85}$$

$$H = \frac{1}{2}\mathrm{tr}N = \frac{\kappa_1 + \kappa_2}{2}. \tag{86}$$

These equations show that the physical relationship between the the Okubo-Weiss field and the magnitude of the vorticity is attributable to simple geometric relationships. That is, if $K > 0$, κ_1 and κ_2 have the same sign. In contrast, κ_1 and κ_2 have opposite signs if $K < 0$. Therefore, $|H|$ in the $K > 0$ regions may be larger compared to $|H|$ in the $K < 0$ regions.

From (1), the Okubo-Weiss field is a comparison between the square of the strain rate, σ, and the vorticity, ω. The geometric expressions of σ^2 and ω^2 are given by $4(H^2 - K) = (\kappa_1 - \kappa_2)^2$ and $4H^2 = (\kappa_1 + \kappa_2)^2$, respectively. Thus, the Okubo-Weiss field can be interpreted as a comparison between the difference of the principal curvatures and their sum.

4.2. Gaussian curvature and mean curvature in the flow

(14) showed that $K = -Q$, and (15) showed that $2H = -\omega$. If the entire area within the irrotational region ($\omega = 0$) is neutral ($Q = 0$), its stream-function surface is a flat ($K = 0$), minimal surface ($H = 0$). That is, the stream-function surface of general flow, in which the coherent (or incoherent) regions and the vorticity normally exist, deviates from the flat, minimal surface. This deviation can be characterized by the Gaussian curvature and the mean curvature.

The mean curvature is extrinsic, *i.e.*, it is defined for the stream-function surface, $\psi(x, y)$, embedded in the space $\mathbb{R}^3$. Therefore, the mean curvature depends on the

embedding. In contrast, the Gaussian curvature is intrinsic, *i.e.*, it can be defined without reference to $\mathbb{R}^3$. Therefore, if two flows have equal Q distributions but different ω distributions, their surfaces, $\psi(x, y)$, have the same intrinsic structure but different extrinsic structures. Thus, we could not distinguish the two flows without reference to higher dimensional space $\mathbb{R}^3$.

In this study, we primarily focused on potential flows (Sections 3.1 and 3.2). Because the mean curvature vanishes in potential flow, it is not necessary to note the embedding of $\psi(x, y)$ in $\mathbb{R}^3$. Therefore, the geometric analysis of potential flow is relatively easy. In contrast, the combined vortex discussed in Section 3.4 showed that the mean curvature inside the core did not vanish (*i.e.*, non-potential flow). Therefore, when we cross the boundary of the core, we observe a change in the intrinsic structure as well as the embedding of $\psi(x, y)$. In general, equation (15): $2H = -\omega$ shows that the extrinsic structure of the stream function changes at the transition between the potential flow and non-potential flow. In other words, we cannot identify the transition without reference to $\mathbb{R}^3$.

4.3. Geometric structure of potential flow

In Section 3.1.1, we calculated the curvature of the stream function for uniform flow. Because this is the simplest flow, its result was used as the standard for analyzing more complex flows. The stream-function surface for uniform flow is planar. Therefore, the stream function for complex flows can be interpreted geometrically as the "deformation" of the planar region. Next, we discuss the curvature related to non-uniform flows, *i.e.*, the deformation of the planar region.

In Sections 3.1.3 and 3.1.4, we calculated the Gaussian curvatures of the stream functions for the source-sink and the point vortex. The comparison between the curvatures (40) and (43), except for the point $(x, y) = (0, 0)$, showed that the two curvatures became equal when the flow rate, m, was replaced by the circulation, Γ. Thus, the stream functions for the source-sink and the point vortex had the same geometric structure with respect to the Gaussian curvature. This can be inferred as follows: (i) from (38) and (41), the velocity potential of the source-sink corresponds to the stream function of the point vortex; and (ii) the stream function and the velocity potential have the same Gaussian curvature (Section 2.2.2). The sign of the flow rate, m, determines the direction of the radial flow, and the sign of the circulation, Γ, determines the direction of the rotation. Because the Gaussian curvature, K, in the potential flow should be non-positive due to $H = 0$, the direction of the potential flow should not change the negative sign of K. In fact, (40) and (43) showed that m and Γ do not change the structure of K or its sign. Therefore, it can be concluded that the stream functions for the four flows, the source, the sink, clockwise motion, and counterclockwise motion, can be classified into the same geometric group based on the mean and Gaussian curvatures.

On the other hand, the stream functions given by the power law potential (Section

3.1.2) were classified into different groups according to the value of n, which corresponds to the angle of the corner flow, as follows. For instance, (37) showed that the local dependence of the curvature vanished when n is one or two, *i.e.*, the angle is π (uniform flow) or $\pi/2$. These two values are critical for corner flow. When $n > 1$, the sign of $\partial_n K$ switches from positive to negative. In this case, the velocity at the origin ($(x, y) = 0$) is given by (i) ∞ for $n < 1$; (ii) A for $n = 1$; and (iii) 0 for $n > 1$. In real fluids, when $n > 1$, the flow downstream of the corner separates from the boundary. When $n > 2$, the proportional relationship between K and $r = \sqrt{x^2 + y^2}$ inverts. In this case, the curvature (*i.e.*, velocity change) at the origin is given by (i) $-\infty$ for $n < 2$; (ii) $-4A^2$ for $n = 2$; and (iii) 0 for $n > 2$. In summary, K shows the same structure in the basic potential flows whose streamlines perpendicularly intersecting or being parallel to each other.

4.4. Geometric stability of the vortex street

As described in Section 2.1, the relationship between the Gaussian curvature of the stream function and the linear stability of the trajectory of particles immersed in 2D flow depends on the relationship between the velocity and the stream function,

$$u = \frac{dx}{dt} = \partial_y \psi, \tag{87a}$$

$$v = \frac{dy}{dt} = -\partial_x \psi. \tag{87b}$$

On the other hand, the motion of point vortices in an incompressible 2D fluid are governed by the same equations, with (87*a*) and (87*b*). This implies that the Gaussian curvature could be useful for diagnosing the linear stability of an array of point vortices. Thus, we discuss the stability of an array of point vortices, in particular, the single and double vortex streets discussed in Section 3.3, by noting the sign of the Gaussian curvature. Note that the linear stability of the vortex street in terms of Gaussian curvature indicates the stability of the position of a point vortex with respect to infinitesimal perturbations applied to the vortex of interest. On the other hand, the well-known linear stability analysis of a vortex street indicates the stability of the array of vortices with respect to infinitesimal sinusoidal perturbations applied to the vortex street [25]. Therefore, it is expected that the stability analyses of the vortex streets by the Gaussian curvature and the well-known analysis would lead to different conclusions. However, it is valuable to compare these two analyses.

4.4.1. Single vortex street As described in Section 3.3.1, the Gaussian curvature at the position of point vortices in the single vortex street is given by (66). Because $K < 0$, *i.e.*, $Q > 0$, a vortex in the single vortex street is unstable to perturbations applied to the vortex of interest. On the other hand, from the well-known analysis, the single vortex street is a linearly unstable arrangement because sinusoidal perturbations applied to the vortex arrangement increase exponentially with time [25]. Thus, both analyses lead to the same conclusion for the single vortex street.

4.4.2. Double vortex street We focused on two cases: the symmetric arrangement ($c = 0$) and the staggered arrangement ($c = b/2$). The symmetric arrangement of the double vortex street is a linearly unstable arrangement because a small sinusoidal perturbation applied to the vortex arrangement increases exponentially with time. The staggered arrangement of the double vortex street is also a linearly unstable arrangement, except for $\cosh(\pi d/b) = \sqrt{2}$. For the case of $\cosh(\pi d/b) = \sqrt{2}$, *i.e.*, $d/b \approx 0.281$, the arrangement is neutral because a small sinusoidal perturbation applied to the vortex arrangement does not change with time [25].

The Gaussian curvature at the position of point vortices, (77), is rewritten as

$$K = -\left|\frac{i\Gamma\pi}{2b^2}\left(\cosh\frac{2\pi d}{b} \pm 5\right)\left(\cosh\frac{2\pi d}{b} \mp 1\right)\right|^2, \tag{88}$$

where the upper and lower signs for $c = 0$ and $c = b/2$, respectively. Because the cosh function is positive and $\cosh(2\pi d/b) > 1$, the Gaussian curvature at the position of point vortices for $c = 0$ is negative; thus, a point vortex within the symmetric arrangement of the double vortex street is unstable with respect to linear perturbation applied to the vortex of interest. In this sense, both analyses lead to the same conclusion for the symmetric arrangements of the double vortex street. In contrast, in the case of $c = b/2$, (77) becomes zero for $\cosh(2\pi d/b) = 5$, *i.e.*, $d/b \approx 0.37$. This indicates that a vortex in the staggered arrangement of the double vortex street is neutral to a perturbation applied to the vortex of interest for the case of $\cosh(2\pi d/b) = 5$.

4.5. Conformal mapping and curvature

Since the method of conformal mapping is particularly useful for the derivation of complicated flow patterns from a known simple flow pattern, this mapping has been widely applied in fluid mechanics. Then, in this section, we discuss the relationship between conformal mapping and the geometric structure of the stream-function surface.

In the conformal mapping of $F : \zeta \to z$, the complex function in the $z = x + iy$ plane has a corresponding complex function in the $\zeta = \xi + i\theta$ plane:

$$z = F(\zeta). \tag{89}$$

Because F is analytic, the conformal mapping is isogonal, *i.e.*, it preserves the magnitudes of local angles between equipotential and streamlines. This property is an advantage for applying the method of conformal mapping to potential-flow problems.

The conformal mapping in fluid mechanics is interpreted as a mapping to derive complicated potential flow from a known simple potential flow. Because the vorticity of potential flows is zero, the Okubo-Weiss field (1) remains non-negative after applying a conformal mapping. Using the relations (14) and (15), the above properties of the conformal mapping can be rewritten geometrically as follows:

(i) The Gaussian curvature remains non-negative after applying a conformal mapping.

(ii) The mean curvature remains zero in the conformal mapping.

Generally speaking, the Gaussian curvature does not change sign by conformal mapping in differential geometry. Thus, the property (i) holds true in general. Moreover, since the mean curvature is a geometrical object, the property (ii) is clear. In summary, conformal mapping in fluid mechanics is physical expression of the geometric facts (i) and (ii). This result implies that the sign of the Okubo-Weiss field is a topological quantity. This invariance property is important since one is often interested in perturbations and structural stability of elementary stream functions.

5. Conclusions

We have discussed the differential geometric structure of the stream function, ψ, for incompressible 2D fluid. The following conclusions were drawn from the results and discussion.

I) As pointed out by Weiss [16], the Gaussian curvature, K, of ψ corresponds to the Okubo-Weiss field Q. Moreover, we showed that the mean curvature, H, of ψ corresponds to the vorticity, ω. Therefore, ψ for potential flows is the minimal surface ($H = 0$ and $K \neq 0$), and ψ for parallel shear flow is one of the developable surfaces ($H \neq 0$ and $K = 0$). In differential geometry, it is well known that a surface can be characterized by the mean and Gaussian curvatures. Therefore, the correspondences found by Weiss [16] and this study suggest that the stream-function surface can be characterized by the vorticity and the Okubo-Weiss field.

II) The relationship between the coherency and the magnitude of the vorticity was attributed to the simple geometric fact that $|H|$ is related to the sign of K.

III) Using the Gaussian curvature, stability of single and double point vortex streets is analyzed. It is derived that the single and symmetric double point vortex streets are unstable arrangements. This is consistent with the well-known linear stability analysis. In contrast, it is derived that the staggered double point vortex street is unstable arrangements except for a particular aspect ratio. This point is also consistent with the well-known linear stability analysis. However, the aspect ratio in the both analysis are inconsistent.

IV) In conformal mapping, the transition from irrotational flow to rotational flow is prohibited. This was attributed to the geometric fact that the sign of K does not change in conformal mapping.

The author's outlook regarding future study is as follows. (i) In the section 4.5, we consider the geometrical structure of the stream function in conformal mapping. In modern conformal geometry, the integral of Branson's Q curvature has been known as a fundamental quantity to derive the invariant quantity in conformal mapping [26–28]. Branson's Q curvature is essentially the Gaussian curvature in 2D space. Therefore, the integral of K of the (compact) stream-function surface, that has not been studied in this paper, is expected to relate to the invariant quantity in the conformal mapping. (ii) In this paper, we did not focus on the geometric evolution of the stream-function surface. To propose a relationship between time and the geometric objects of the stream-

function surface, we should introduce the Navier-Stokes equations for incompressible 2D flow. From the results of this paper, the equation without the pressure in terms of the metric g_{ij} of the stress-function surface is diffusion equation with nonlinear term: $\partial_t\sqrt{g_{ii}} = \nu\triangle\sqrt{g_{ii}} - \sqrt{g_{jj}}\,\partial_k\sqrt{g_{ii}}$, where $v_i = \sqrt{g_{ii}}$ (the summation convention is not used), $v_x = v$, $v_y = u$ and ν is the coefficient of kinematic viscosity. It is interesting to develop this point of view because nonlinear diffusion equation for metric is of considerable concern in the modern differential geometry. §

References

[1] Kröner, E 1981. Continuum theory of defects *Physics of Defects* ed. R Balian, M Kleman and J-P Poirier (Amsterdam: North-Holland) pp 214-315.

[2] Edelen, D G B and Lagoudas, D C 1988 *Gauge Theory and Defects in Solids* (Amsterdam: North-Holland).

[3] Kleinert, H 1989 *Gauge Fields in Condensed Matter* vol. 2 (Singapore: World Scientific).

[4] Yamasaki, K and Nagahama, H 1999 *J. Phys. A: Math. Gen.* **32** L475.

[5] Yamasaki, K and Nagahama, H 2002 *J. Phys. A: Math. Gen.* **35** 3767.

[6] Edelen, D G B 2005 *Applied Exterior Calculus* (New York: Dover).

[7] Miklashevich, I A 2008 *Micromechanics of Fracture in Generalized Spaces* (London: Academic Press).

[8] Agiasofitou, E and Lazar, M 2010 *J. Elasticity* **99** 163.

[9] Teisseyre, R 1995. Dislocations and cracks: Earthquake and fault models: Introduction *Theory of Earthquake Premonitory and Fracture Processes* ed. R Teisseyre (Warszawa: PWN) pp 131-135.

[10] Yamasaki, K and Nagahama, H 2008 *Z. Angew. Math. Mech.* **88** 515.

[11] Yamasaki, K 2009 *Acta Geophys.* **57** 567.

[12] Ebin, D G and Marsden, J 1970 *Ann. Math.* **92** 102.

[13] Taylor, M E 1996 *Nonlinear Equations* (New York: Springer-Verlag).

[14] Arnol'd, V I and Khesin, B A 1998 *Topological Methods in Hydrodynamics* (New York: Springer-Verlag).

[15] Fischer, A E 2004 *Classical Quantum Gravity* **21** S171.

[16] Weiss, J 1991 *Physica* D **48** 273.

[17] Lukovich, J V and Barber, D G 2009 *J. Geophys. Res.* **114**, D02104.

[18] Cruz Gømez, R C and Bulgakov, S N 2007 *Ann. Geophys.* **25** 331.

[19] Benzi, R; Patarnello, S; and Santangelo, P 1988 *J. Phys. A* **21** 1221.

[20] Okubo, A 1970 *Deep-Sea Res.* **17** 445.

[21] Gray, A; Abbena, E; and Salamon, S 2006 *Modern Differential Geometry of Curves and Surfaces with Mathematica* (3rd ed.) (Boca Raton: Taylor and Francis).

[22] Drazin, P G and Reid, W H 1981 *Hydrodynamics Stability* (Cambridge: Cambridge Univ. Press).

[23] Munson, B R; Young, D F; Okiishi, T H; and Huebsch, W W 2010 *Fundamentals of Fluid Mechanics* (6th ed.) (Hoboken, N.J: Wiley).

[24] Iwayama, T and Okamoto, H 1996 *Prog. Theor. Phys.* **96** 1061.

[25] Karman, T Von 1911 *Gott. Nachr., Math. Phys. Kl.* **12** 509.

[26] Branson, T P and Ørsted, B 1991 *Proc. Am. Math. Soc.* **113** 669.

[27] Baum, H and Juhl, A 2010 *Conformal Differential Geometry* (Berlin: Birkhauser).

[28] Chang, S-Y A 2005 *Bull. Amer. Math. Soc. (N.S.)* **42** 365.

§ For instance, the Ricci flow equation in harmonic coordinates is given by $\partial_\tau\widetilde{g}_{ij} = \triangle\widetilde{g}_{ij} + \widetilde{g}^{-1}\star\widetilde{g}^{-1}\star\partial\widetilde{g}\star\partial\widetilde{g}$, where τ is the variable for time in differential geometry, $\widetilde{g}_{ij}$ is Riemannian metric and $\widetilde{g}^{-1}\star\widetilde{g}^{-1}\star\partial\widetilde{g}\star\partial\widetilde{g}$ denotes a sum of contractions [29, 30].

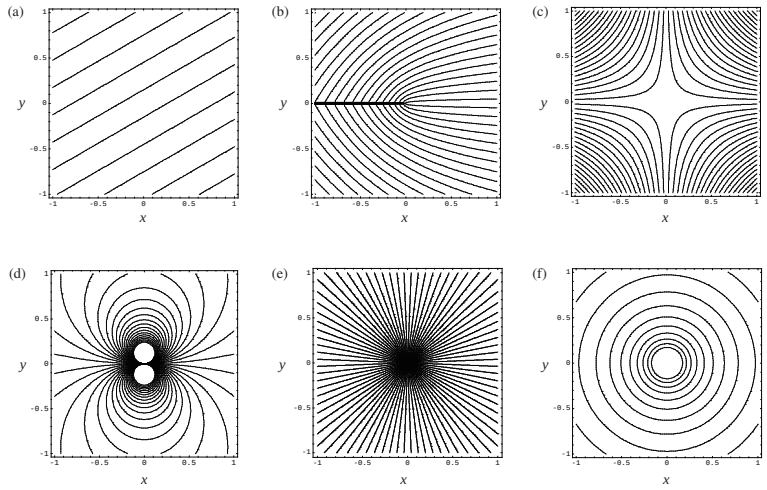

Figure 1. Streamlines for basic flows. (a) Uniform flow: $U = 1$ and $\alpha = \pi/6$. (b) Flow in the vicinity of the $(3/2)\pi$ corner: $A = 1$ and $n = 2/3$. (c) Flow in the vicinity of the $(1/2)\pi$ corner: $A = 1$ and $n = 2$. (d) Doublet: $A = 1$ and $n = -1$. (e) Radial flow: $|m| = 1$. (f) Point vortex: $|\Gamma| = 1$.

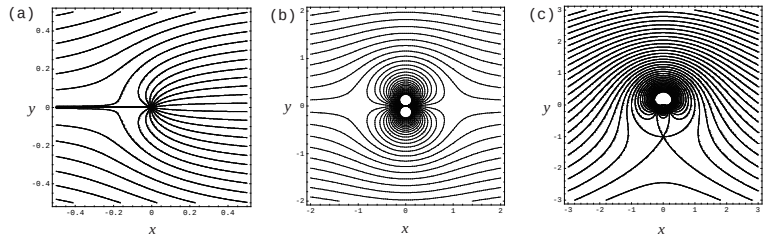

Figure 2. Streamlines for combined flows. (a) Flow around a half-body: $U = m = 1$. (b) Flow around a circular cylinder: $U = A = 1$. (c) Flow around a rotating cylinder: $U = a = 1$ and $\Gamma = 4\pi$.

655 [29] Hamilton, R S 1982 *Jour. Diff. Geometry* **17** 255.
656 [30] Chow, B and Knopf, D 2004 *The Ricci flow: An introduction* (Providence, R.I.: American
657 Mathematical Society).

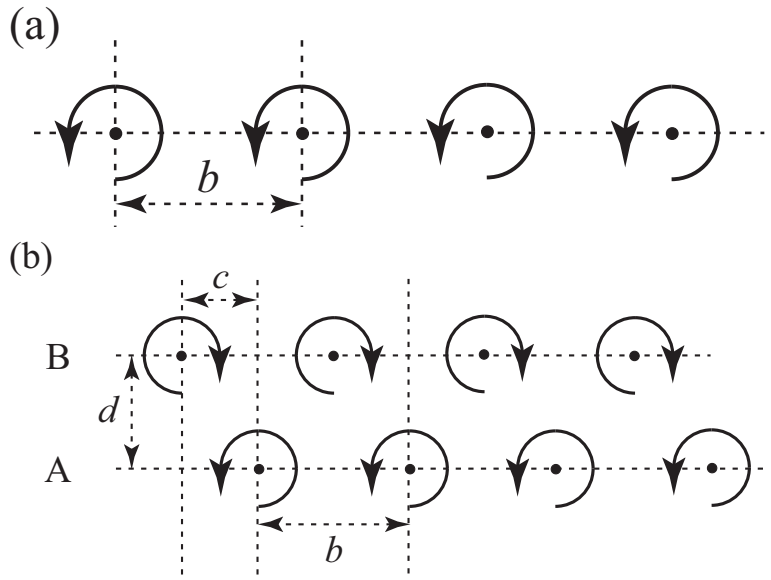

Figure 3. (a) Single vortex street. (b) Double vortex street.